Eur Biophys J (2008) 37:1229–1233
DOI 10.1007/s00249-008-0342-8

ORIGINAL PAPER

Flow-induced permeation of non-occlusive blood clots: an MRI study and modelling

Barbara Grobelnik · Jernej Vidmar · Gregor Tratar · Aleš Blinc · Igor Serša

Received: 12 September 2007 / Revised: 22 April 2008 / Accepted: 28 April 2008 / Published online: 14 May 2008

Abstract The success of clot thrombolysis very much depends on efficient clot permeation with blood plasma carrying the thrombolytic agent. In this paper clot permeation was studied by dynamic magnetic resonance imaging (MRI) on artificial non-occlusive blood clots inserted in an artificial circulation system filled with blood plasma to which an MRI contrast agent was added. The MRI results revealed that clot permeation is much faster and more efficient at the entrance of the flow channel across the clot. Clot permeation with fluid was simulated numerically as well. The simulation was based on numerical solution of Navier–Stokes equations for the flow in the channel and within the clot. The clot was considered as a porous material with known permeability and porosity. Based on the calculated velocity profiles, concentration profiles of fluid in the clot were modelled. These agreed well with the MRI results. The presented model of clot permeation with fluid may also serve as a useful extension to numerical modelling of dissolution of non-occlusive blood clots during thrombolytic therapy.

Regional Biophysics Conference of the National Biophysical Societies of Austria, Croatia, Hungary, Italy, Serbia, and Slovenia.

B. Grobelnik · J. Vidmar · I. Serša (✉)
Jožef Stefan Institute, Jamova 39,
1000 Ljubljana, Slovenia
e-mail: igor.sersa@ijs.si

G. Tratar · A. Blinc
Department of Vascular Diseases,
University of Ljubljana Medical Centre,
1000 Ljubljana, Slovenia

Keywords Flow · Permeation · Thrombolysis · Non-occlusive blood clot · Mathematical modelling · Dynamical MRI

Introduction

Thrombolytic therapy aims to dissolve blood clots and restore vessel patency. It is used in treatment of ischaemic stroke (White-Bateman et al. 2007), pulmonary embolism (Kucher and Goldhaber 2006) and acute arterial thrombosis (Kandarpa 1999). Thrombolysis starts with activation of the proenzyme plasminogen into the active serine protease plasmin (Collen 1999) that is very efficient in degrading the fibrin network. During thrombolytic treatment, activation of plasminogen is achieved by adding a thrombolytic agent to the circulation. Recombinant tissue type plasminogen activator (rt-PA) is a widely used fibrin-specific thrombolytic agent that excels in its ability to activate only the plasminogen in contact with the fibrin network. One of the major problems in thrombolysis is efficient and fast transport of the thrombolytic agent into the clot. Diffusion, as a mode of thrombolytic agent transportation, is very slow (Blinc and Francis 1996); and for this reason the dissolution of occlusive blood clots is slow and inefficient unless a pressure gradient drives convective flow through the porous clot. The dissolution is much faster in non-occlusive blood clots exposed to a flow channel with an established fast, axially directed blood flow. In the latter case, dissolution is faster for two reasons: firstly, the thrombolytic agent is delivered to the clot by convection, which is a significantly faster process than diffusion, and secondly, the blood flow exerts large mechanical forces on the surface of the clot that act is parallel with the biochemical processes and help in

degrading the clot more efficiently (Sakharov and Rijken 2000; Sersa et al. 2007a).

Our recent results (Sersa et al. 2007b) of dynamic 3D magnetic resonance imaging (MRI) of blood clot dissolution in an artificial circulation system showed that non-occlusive blood clots dissolve non-uniformly. The dissolution is considerably faster at the entrance of the flow channel than further downstream. The effect is considerable within the entrance distance of approximately one tenth of the entrance length (Nichols et al. 2005). The faster dissolution may be attributed to the higher shear velocity at the entrance and therefore larger viscous forces to the clot surface. However, present results indicate that the dissolution is also faster due to better permeation of the clot with the plasma carrying the thrombolytic agent. This effect was studied by dynamic MRI of clots in artificial circulation.

Materials and methods

Artificial whole blood clots were prepared in 3 cm long glass tubes 3 mm in diameter, as described previously (Tratar et al. 2004). The procedure was the following: citrated venous blood was clotted by addition of thrombin and calcium, and clot retraction was inhibited by the phosphodiesterase inhibitor UDCG 212 (Boehringer, Germany). After at least an hour at room temperature to allow for fibrin formation, a hole of 0.7 mm diameter was made in the clot lengthways by a needle to create a flow channel (Fig. 1a). The glass tube containing the clot was connected by a flexible hose to a peristaltic pump that generated a constant flow rate of 2 ml/min through the clot. The hose connecting the pump and the clot was 1.7 m long and also had a 3 mm inner diameter. The artificial circulation system in each experiment was filled with approximately 0.5 l of blood plasma at room temperature to which was added the magnetic resonance contrast agent Gd-DTPA (Magnevist, Berlex Lab., Germany) at 1 mmol/l. The magnetic resonance contrast agent, in a concentration that can be well seen on T1-weighetd MR images, was used to mark the water phase that carries the thrombolytic agent. In spite of the differences in molecular weight (Gd-DTPA, mol. wt. 590 Da and rt-PA, mol. wt. 68 kDa) it was assumed that both permeate in the clot similarly, since pores in the fibrin network are of micrometre dimensions and thus much larger than the diameters of either molecule. The concentration at which Gd-DTPA was added to the circulation system enabled good visual discrimination between non-permeated and completely permeated parts of blood clots.

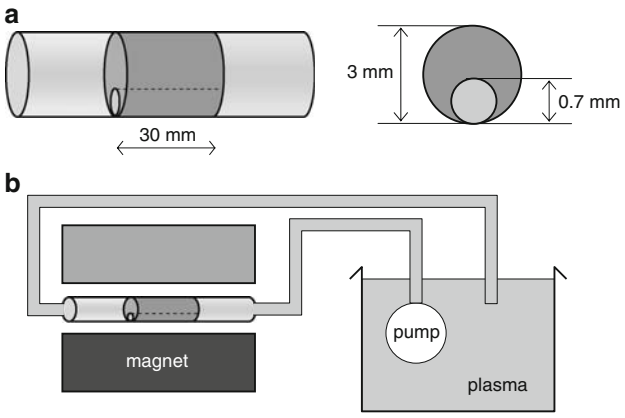

Fig. 1 Non-occlusive blood clot (**a**) and the circulation system used for clot permeation imaging (**b**)

The dynamics of Gd-DTPA permeation into the clot was measured by dynamic magnetic resonance microscopy. Clots in glass tubes were inserted into a 25 mm radio-frequency probe and connected to the artificial circulation system (Fig. 1b). Before adding Gd-DTPA to the plasma, the flow system was tested for stability, assuring that there were no air bubbles in the system which could obstruct the plasma flow. Then, the probe with the clot was inserted into a 100 MHz (proton frequency) horizontal bore Oxford superconducting NMR magnet equipped with a Bruker micro-imaging gradient system with maximum gradients of 300 mT/m. The magnet and the gradients were controlled by a TecMag NMR/MRI spectrometer. When the flow was stable and the clot was in the magnet, Gd-DTPA was added to the plasma and dynamic imaging was started. Blood clots were imaged by the Rapid acquisition relaxation enhancement (RARE) method (Hennig et al. 1986) in the sagital central slice across the clot. The imaging parameters were as follows: field of view (FOV) 15 mm, image matrix 256 by 256, slice thickness (SLTH) 4 mm, interecho time 6 ms, echo train length (ETL) 8, repetition time (TR) 1,100 ms; a sequential (standard spin warp) acquisition order was used. In 18 min 30 images were acquired; one every 36 s. Although the parameters are not typical of the standard T1-weighted image, the image contrast between Gd-DTPA permeated regions of the clot and those without it was very good.

Permeation of the water phase, delivering the drug into the blood clot, was modelled as well. The modelling was done for 2D geometry in which a 3 mm wide channel (normal blood vessel) in the position of a 3 cm long and 2.3 mm thick clot was constricted to a 0.7 mm wide flow channel (Fig. 2a). The initial condition was a flat plasma velocity profile of 5 mm/s in the initial channel which attained a parabolic velocity profile until reaching the clot 30 mm downstream of the entrance. The flow of plasma and its permeation into the clot was solved numerically using the Fluent computer program (Fluent Inc., Lebanon NH, USA), which solved Navier–Stokes equations of flow (Landau and Lifshitz 1995)

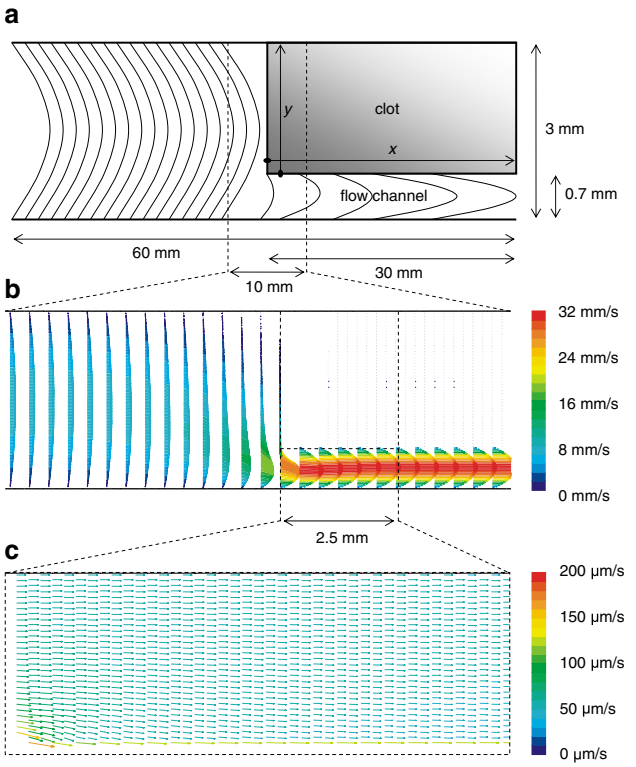

Fig. 2 Geometry of the flow channel with the clot in the 2D model (**a**) and corresponding calculated velocity vector maps of plasma flow in the entrance to the flow channel (**b**) and plasma permeation in the clot (**c**). The velocity maps were calculated numerically using Navier–Stokes equations (flow in the channel) and their modification for flow in porous media (permeation in the clot)

$$\rho\left(\frac{\partial v}{\partial t}+(\vec{v}\cdot\nabla)\vec{v}\right)=-\nabla p-\frac{\mu}{\alpha}\vec{v}+\mu\nabla^2\vec{v}$$
$$\frac{\partial\rho}{\partial t}+\nabla\cdot(\rho\vec{v})=0. \quad (1)$$

The term $-(\mu/\alpha)\vec{v}$, in Eq. (1), corresponds to the flow resistance in the porous media. The term is zero everywhere except in the clot, where, due to the low clot permeability, it practically entirely compensates the pressure gradient. In the model, the clot was considered as a porous material with the permeability of $\alpha = 10^{-10}$ m^2 (Carr et al. 1977) into which plasma permeates with a viscosity $\mu = 0.0018$ Pas and density $\rho = 1035$ kg/m^3. The output of the program was a plasma flow velocity map in the channel and its permeation velocity map $\vec{v}(x,y)$ in the clot. The latter was used to calculate drug concentration profiles in the clot as a function of time. The profiles were obtained by integration of the 2D permeation map, of which just the x-velocity component was considered (Fig. 2a). At time $t = 0$, a constant drug concentration was assumed at the $x = 0$ flank of the clot. The profiles were then calculated iteratively, i.e., for each y component a new depth of the permeation front x_{i+1} corresponding to time $t = (i + 1)\,\Delta t$ was calculated from the previous depth x_i (at time $t = i\,\Delta t$) using the equation

$$x_{i+1}(y) = v(x_i(y))\Delta t. \quad (2)$$

Results and discussion

Solutions of the Navier–Stokes equation for the plasma flow in the channel and its perfusion of the clot are shown in Fig. 2. The clot and channel geometry in the 2D model are depicted in Fig. 2a. In the initial non-occluded channel, before entering the narrowed flow channel through the clot, plasma had a parabolic velocity profile with an average velocity of 5 mm/s that progressively changed into another parabolic velocity profile in the narrowed channel with a much faster flow (Fig. 2b). In that section, due to conservation of flow, the average velocity increased to 21.4 mm/s due to the 4.3 times reduction of the channel width. At the entrance to the narrowed flow channel, the flow was not fully developed and its shape was not parabolic. A fully developed flow, with a parabolic velocity profile, developed after the entrance distance, which is approximately equal to 0.06 times the Reynolds number times the channel width (Nichols et al. 2005). In our experiment the entrance distance was equal to 0.4 mm. This also agree well with the velocity vector field simulation in Fig. 2b that shows a 10 mm long segment centred on the clot entrance.

The plasma flow around the clot also determines its permeation into the clot. In addition, the plasma permeation is also very much determined by the porous properties of the clot, mainly by its permeability. As blood clots have a relatively small permeability constant, the plasma permeation velocity in the clot is much smaller than its flow velocity in the channel. In the permeation simulation shown in Fig. 2c the average permeation velocity was 50 μm/s, which was more than 400 times less than the flow velocity in the narrowed flow channel. The simulation in Fig. 2c shows just the initial 2.5 mm long segment of the clot in which permeation velocity profiles were not yet fully developed. In that section, a small plasma leakage from the clot back to the narrowed flow channel was present. This can be seen from the velocity vectors that were slightly declined from the axial direction towards the channel. Because of the plasma leakage the permeation velocity slightly decreased in the proximity of the channel and again increased in the very narrow region next to the channel, due to viscous forces of the streaming plasma in the flow channel. This effect can be best seen in profiles of the permeation velocity magnitude in Fig. 3, which are plotted for various entrance distances. The profile at the entrance point (blue curve, 0 mm) has the highest velocity of all the profiles. It decreases as an exponential-like function towards the terminal velocity of 60 μm/s reached

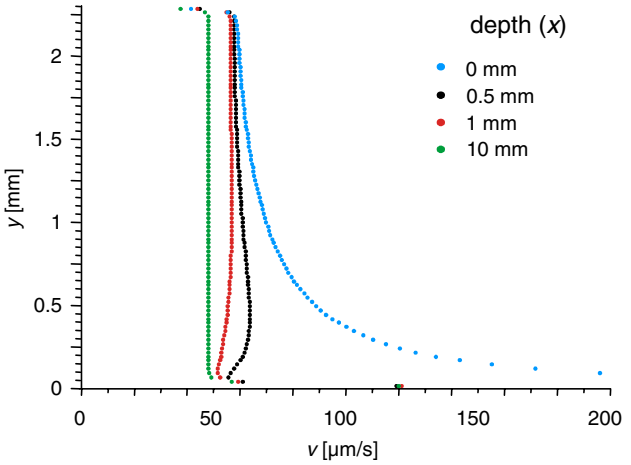

Fig. 3 Velocity profiles of plasma permeation in the clot plotted for different entrance distances (x). The velocity magnitude, calculated from the permeation velocity vector map in Fig. 2c, is plotted as a function of the normal distance from the channel (y)

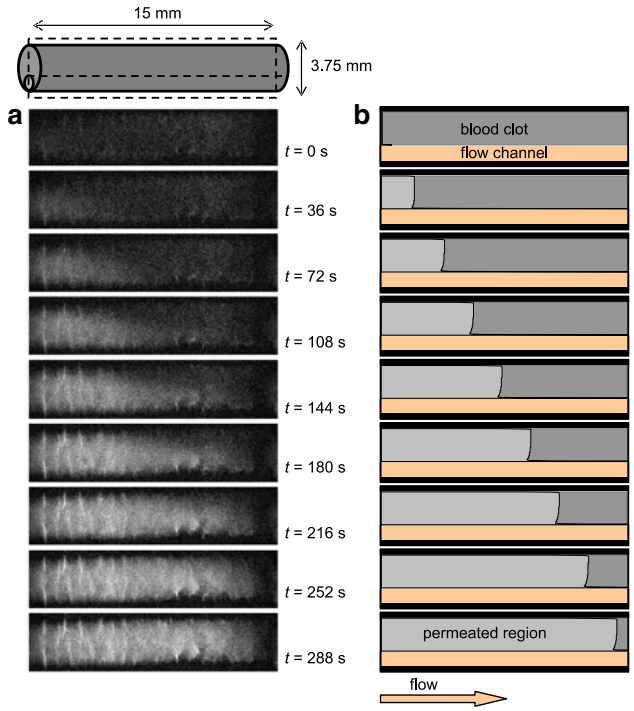

Fig. 4 Dynamic MRI measurements of clot permeation with the MRI contrast agent Gd-DTPA that mimics clot permeation with plasma carrying the thrombolytic agent during thrombolytic therapy (**a**) and numerical simulation of the same process (**b**). MRI images of the clot in sagital orientation are T1-weighted so that the clot appears *dark grey* and the region permeated by Gd-DTPA appears light grey. MR images (**a**) show just the clot without the flow channel. The flow channel is not visible on the MR images due to fast plasma flow

in the proximity of the vessel-clot interface. For larger entrance distances (black and red curves, 0.5, 1 mm) the profile is practically uniform except in the proximity of the clot-channel interface, where a slight velocity decrease appears. The profile at 10 mm entrance distance (green) is flat as well, but its velocity decreases to 50 μm/s due to leakage of plasma in the channel. For entrance distances larger than 1 cm, all profiles are practically identical.

Dynamic 2D MR images of permeation of the MRI contrast agent (Gd-DTPA) into the clot (Fig. 4a) agree well with the calculated progression of the permeation front in the clot (Fig. 4b). The front was calculated from the simulated permeation velocity (Figs. 2c and 3) using the iterative formula in Eq. (2). Bright clot regions in the MR images correspond to regions with a high contrast agent concentration. Assuming that thrombolytic agents, like rt-PA, have similar migration properties as the Gd-DTPA molecule, the Gd-DTPA permeated regions would also correspond to regions well permeated with the thrombolytic drug.

The use of the MRI contrast agent Gd-DTPA is of course not a very good surrogate for the larger molecules of rt-PA (590 Da vs. 68 kDa) which also binds to the fibrin network. However, both molecules are water soluble, and the Gd-DTPA molecule, with a size of a few Å, as well as the rt-PA molecule, with a size of a few nm, are both much smaller than the pores between the fibrin strands of the clot which are typically of μm dimensions. Therefore, it may be assumed that the migration of both molecules is governed mainly by the flow of plasma in the porous clot and is not so much influenced by the size of the molecules nor their concentration. The permeation velocity profiles determined by Gd-DTPA should also hold for larger molecules of rt-PA size. This applies to all neutral molecules that do not bind to fibrin. Since rt-PA binds to fibrin, its concentration may be higher close to surfaces exposed to streaming plasma than deeper in the clot. rt-PA concentration may decay exponentially towards the clot interior because of binding to fibrin. The extent of this effect could be investigated by designing an rt-PA-like MRI contrast agent. The molecule should have the fibrin binding properties of rt-PA, its molecular mass and a strong paramagnetic centre so that it could enhance MRI contrast. With such a new contrast agent, rt-PA permeated regions could be defined precisely and the permeation model redefined by inclusion of drug binding to fibrin.

Better permeation of the clot with the thrombolytic agent at the entrance of the flow channel favours of faster clot dissolution in that region. This was in fact observed in our previous clot dissolution MRI experiments (Sersa et al. 2007b) in which clot dissolution in an artificial circulation system was dynamically imaged by the 3D RARE MR imaging method. The 3D images of clots were then analysed by measuring the flow channel area as a function of the entrance distance. Faster clot dissolution was observed in the first few millimetres downstream from the entrance point. The faster clot dissolution at the entrance of the flow

channel was explained as a consequence of larger shear velocities due to flow separation and with the associated larger mechanical forces on the surface of the clot in that region. Based on the results in Fig. 4, we are convinced that better permeation of the clot with the thrombolytic agent at the entrance point may contribute to the faster dissolution of the clot in that region as well.

Due to the complex geometry we were not able to solve the Navier–Stokes equations for flow in the clot channel and clot permeation analytically. An analytical solution could be directly included in our analytical model for clot dissolution presented in (Sersa et al. 2007a, b). Our present model does not include the effect of spatial and time dependent permeation of the clot with the thrombolytic agent. It simply assumes that the clot is uniformly permeated with the thrombolytic agent at the beginning of the dissolution process and that the thrombolytic agent becomes active after a time delay, and that activation is not abrupt but rather gradual. Nevertheless, the presented numerical simulation approach for clot permeation with the thrombolytic agent may be further extended to the dissolution model by incorporating the biochemical clot degradation properties of the thrombolytic agent and the effect of viscous forces due to shearing of blood. Such models have been successfully applied for studying post-canalization thrombolysis in low-velocity flow (Pleydell et al. 2002) and for thrombolysis of mural clots (Wootton et al. 2002). The numerical approach has also other advantages, such as more accurate modelling of the clot and the flow channel geometry, and inclusion of flow pulsation in the model.

Conclusion

Modelling of clot permeation with plasma carrying the thrombolytic agent can help in understanding the dynamics of clot dissolution better. The result of MRI experiments showed that non-occlusive blood clots are permeated with plasma carrying the thrombolytic agent at the entrance of the flow channel more efficiently and faster than further downstream. This result partially explains why clots dissolve faster at the entrance to the flow channel than at its exit during thrombolytic treatment. The simulation of clot permeation with the thrombolytic agent agrees well with the experimental MRI results. The simulation of clot permeation represents a valuable extension to our existing model of clot dissolution.

References

Kandarpa K (1999) Catheter-directed thrombolysis of peripheral arterial occlusions and deep vein thrombosis. Thromb Haemost 82:987–996

Blinc A, Francis CW (1996) Transport processes in fibrinolysis and fibrinolytic therapy. Thromb Haemost 76:481–491

Carr ME Jr, Shen LL, Hermans J (1977) Mass-length ratio of fibrin fibers from gel permeation and light scattering. Biopolymers 16:1–15

Collen D (1999) The plasminogen (fibrinolytic) system. Thromb Haemost 82:259–270

Hennig J, Nauerth A, Friedburg H (1986) RARE imaging: a fast imaging method for clinical MR. Magn Reson Med 3:823–833

Kucher N, Goldhaber SZ (2006) Risk stratification of acute pulmonary embolism. Semin Thromb Hemost 32:838–847

Landau LD, Lifshitz EM (1995) Fluid mechanics, 2nd edn. Butterworth-Heinemann, Oxford

Nichols WW, McDonald DA, O'Rourke MF (2005) McDonald's blood flow in arteries: theoretical, experimental, and clinical principles, 5th edn. Hodder Arnold; distributed in the United States of America by Oxford University Press, New York

Pleydell CP, David T, Smye SW, Berridge DC (2002) A mathematical model of post-canalization thrombolysis. Phys Med Biol 47:209–224

Sakharov DV, Rijken DC (2000) The effect of flow on lysis of plasma clots in a plasma environment. Thromb Haemost 83:469–474

Sersa I, Tratar G, Mikac U, Blinc A (2007a) A mathematical model for the dissolution of non-occlusive blood clots in fast tangential blood flow. Biorheology 44:1–16

Sersa I, Vidmar J, Grobelnik B, Mikac U, Tratar G, Blinc A (2007b) Modelling the effect of laminar axially directed blood flow on the dissolution of non-occlusive blood clots. Phys Med Biol 52:2969–2985

Tratar G, Blinc A, Strukelj M, Mikac U, Sersa I (2004) Turbulent axially directed flow of plasma containing rt-PA promotes thrombolysis of non-occlusive whole blood clots in vitro. Thromb Haemost 91:487–496

White-Bateman SR, Schumacher HC, Sacco RL, Appelbaum PS (2007) Consent for intravenous thrombolysis in acute stroke: review and future directions. Arch Neurol 64:785–792

Wootton DM, Popel AS, Alevriadou BR (2002) An experimental and theoretical study on the dissolution of mural fibrin clots by tissue-type plasminogen activator. Biotechnol Bioeng 77:405–419